An rRNA fragment in extracellular vesicles secreted by human airway epithelial cells increases the fluoroquinolone sensitivity of *P. aeruginosa*

Katja Koeppen[1]*, Thomas H. Hampton[1], Scott A. Gerber[2], Young Ah Goo[3], Byoung-Kyu Cho[3], Danielle M. Vermilyea[1], Deborah A. Hogan[1] and Bruce A. Stanton[1]

[1]Department of Microbiology and Immunology, Geisel School of Medicine at Dartmouth, Hanover, New Hampshire, United States of America

[2]Norris Cotton Cancer Center, Geisel School of Medicine at Dartmouth, Lebanon, New Hampshire, United States of America

[3]Mass Spectrometry Technology Access Center, McDonnell Genome Institute, Washington University School of Medicine, St. Louis, Missouri, United States of America

*Corresponding author
E-mail: Koeppen.Katja@gmail.com

Abstract

Lung infection by antibiotic resistant strains of *Pseudomonas aeruginosa* is a well-known concern for immunocompromised hosts including people with lung diseases such as cystic fibrosis. We have previously demonstrated that extracellular vesicles (EVs) secreted by primary human airway epithelial cells (AEC) deliver miRNA let-7b-5p to *P. aeruginosa* where it suppresses biofilm formation and increases sensitivity to beta-lactam antibiotics. In this study we used RNA-seq to characterize the small RNA (sRNA) content of EVs secreted by AEC and demonstrate transfer of multiple distinct RNA fragments from EVs to *P. aeruginosa*. Bioinformatic predictions reveal that several sRNAs may target all three subunits of the fluoroquinolone efflux pump MexHI-OpmD, an effect predicted to increase antibiotic sensitivity to fluoroquinolone antibiotics. Exposure of *P. aeruginosa* to EVs resulted in a significant reduction in the protein levels of MexH (-48%), MexI (-50%) and OpmD (-35%). Moreover, EVs reduced planktonic growth of *P. aeruginosa* in the presence of the fluoroquinolone antibiotic ciprofloxacin by 20%. A *mexGHI-opmD* deletion mutant of *P. aeruginosa* phenocopied this increased sensitivity to ciprofloxacin. Finally, we found that a fragment of an 18S rRNA external transcribed spacer that was transferred to *P. aeruginosa* by EVs was sufficient to reduce planktonic growth of *P. aeruginosa* in the presence of ciprofloxacin, to reduce the minimum inhibitory concentration (MIC) of *P. aeruginosa* for ciprofloxacin by over 50%, and to significantly reduce protein levels of MexH and OpmD. In conclusion, an rRNA fragment secreted by AEC in EVs increases the ciprofloxacin sensitivity of *P. aeruginosa* by targeting and down-regulating the fluoroquinolone efflux pump MexHI-OpmD. A combination of rRNA fragments and ciprofloxacin packaged in nanoparticles or EVs may benefit patients with antibiotic-resistant *P. aeruginosa* infections.

Author Summary

According to the World Health Organization and the U.S. Centers for Disease Control and Prevention the development of antibiotic resistant strains of bacteria, including *Pseudomonas aeruginosa*, are a significant global threat to human health. Thus, development of new approaches to eliminate antibiotic resistant infections is required. In this study, we report that lung epithelial cells secrete extracellular vesicles (EVs) that fuse with and deliver small rRNAs to *P. aeruginosa*, and that the rRNAs increase the sensitivity of *P. aeruginosa* to the antibiotic ciprofloxacin by reducing protein levels of the drug efflux pump MexHI-OpmD. We identified one rRNA fragment that by itself significantly reduced the protein levels of MexH and OpmD and increased the ability of ciprofloxacin to kill *P. aeruginosa*. We propose that developing synthetic vesicles containing a combination of the rRNA that inhibits antibiotic efflux pumps and ciprofloxacin would benefit patients with antibiotic resistant *P. aeruginosa* infections.

Introduction

Pseudomonas aeruginosa is an opportunistic bacterial pathogen that can cause chronic infections in immunocompromised hosts, leading to increased morbidity and mortality in individuals with cystic fibrosis (CF), chronic obstructive pulmonary disease (COPD), ventilator-associated pneumonia and burn wounds (1). *P. aeruginosa* is also emerging as a pathogen that commonly co-infects and exacerbates COVID-19 infections (2–5). The rise of difficult-to-eradicate, antibiotic resistant strains of *P. aeruginosa* is posing treatment challenges and increasingly becoming a concern in healthcare settings (6–9). Multidrug-resistant strains of *P.*

73 *aeruginosa* are estimated to have caused about 32,600 hospital-acquired infections and 2700
74 deaths in the US in 2017 and have been rated as a serious threat by the CDC in a 2019 report
75 (10). Thus, new approaches are needed to eradicate antibiotic resistant infections by *P.*
76 *aeruginosa.*
77 Bi-directional host-pathogen communication through short RNA (sRNA) in extracellular vesicles
78 (EVs) and the resulting regulation of the host immune response as well as bacterial phenotypes
79 such as antibiotic sensitivity have become a research focus in recent years (11–19). We have
80 previously shown that *P. aeruginosa* outer membrane vesicles deliver a transfer RNA (tRNA)
81 fragment to human airway epithelial cells (AEC), suppressing the host innate immune response
82 to infection, thereby facilitating chronic infections (11). Eukaryotic EVs have also been reported
83 to contain tRNA fragments (20–22) and tRNA fragments regulate gene expression in eukaryotes
84 and prokaryotes (23–27), and to play a role in various human diseases (28,29). Previous
85 studies have primarily focused on the regulatory effects of tRNA fragments from a given
86 organism on that same organism, rather than on inter-species crosstalk. Much less is known
87 about the role of tRNA fragments and other sRNAs in inter-kingdom signaling between
88 eukaryotic and prokaryotic organisms.
89 Besides tRNA fragments and messenger RNAs (mRNA), eukaryotic EVs contain a diverse
90 assortment of non-coding RNA species, including long non-coding RNAs (lncRNA), microRNAs
91 (miRNA), piwi-interacting RNAs (piRNA), Y RNAs, antisense RNAs, transfer RNAs (tRNA),
92 tRNA fragments, and ribosomal RNAs (rRNA) (20,22,30–33). EVs as well as their miRNA cargo
93 are involved in immune regulation and their secretion and RNA content have been shown to be
94 dysregulated in patients with airway diseases (34–38). For example, a recent study found that
95 increased levels of miR-223-3p or miR-451a and decreased levels of miR-27b-3p in sputum
96 supernatants correlated with exacerbation in children with CF and infection with *Aspergillus*,
97 *Haemophilus,* or *Pseudomonas*, respectively, suggesting the involvement of EV miRNAs in
98 pulmonary exacerbation (39). Two recent studies provide a comprehensive characterization of

99 the sRNA content of EVs secreted by AEC – one reporting changes in the sRNA content of EVs
100 secreted by the human airway epithelial cell line A549 in response to viral infection (40), and
101 another describing cigarette smoke induced changes in the RNA content of EVs secreted by
102 primary small airway epithelial cells (41). Prior studies of EVs secreted by airway epithelial cells
103 (AEC) have focused mainly on their miRNA cargo (19,42–44), whereas the function of other
104 sRNA species contained in AEC EVs has not yet been reported. While there is a growing body
105 of literature on the regulatory effects of EV sRNAs within a given organism, little is known about
106 the ability of sRNAs secreted in eukaryotic EVs to regulate gene expression in prokaryotes. For
107 example, eukaryotic miRNAs affect the growth of gut microbes through an unknown mechanism
108 (45–47). Recently, we provided the first direct evidence that a miRNA, let-7b-5p, in EVs
109 secreted by human airway epithelial cells, is transferred to *P. aeruginosa,* where it increases
110 beta-lactam antibiotic sensitivity and decreases biofilm formation by reducing the abundance of
111 the beta-lactamase AmpC and several proteins required for biofilm formation (19). Here, we
112 report that human EVs also reduce the abundance of all three subunits of the fluoroquinolone
113 efflux pump MexHI-OpmD and increase fluoroquinolone sensitivity, an effect mediated by an
114 rRNA fragment secreted in EVs.
115
116

117 Results

118

119 EVs increase the fluoroquinolone sensitivity of *P. aeruginosa*

120 In a previous study we demonstrated that EVs secreted by AEC increased the sensitivity of *P.*
121 *aeruginosa* to beta lactam antibiotics by delivering the miRNA let-7b to *P. aeruginosa* (19). To
122 test the hypothesis that EVs may also alter the sensitivity to other antibiotics typically used to

123 treat infections by *P. aeruginosa* (48), we examined the ability of EVs to alter the sensitivity of *P.*
124 *aeruginosa* to the fluoroquinolone antibiotic ciprofloxacin. To that end, the planktonic growth of
125 *P. aeruginosa* strain PA14 as well as the mucoid *P. aeruginosa* CF clinical isolate SMC1585
126 (49) were measured in the presence and absence of EVs and in the presence and absence of
127 eight different concentrations of ciprofloxacin to determine the minimal inhibitory concentration
128 (MIC). EVs alone had no significant effect on planktonic growth of PA14 in the absence of
129 ciprofloxacin (Fig 1A) but reduced the MIC of ciprofloxacin by 25% (Fig 1B). EVs reduced
130 planktonic growth of PA14 in the presence of 0.02 µg/ml ciprofloxacin (corresponding to about
131 one third of the MIC) by 26%, compared to 0.02 µg/ml ciprofloxacin alone (Fig 1C). Likewise,
132 EVs alone had no significant effect on planktonic growth of clinical isolate SMC1585 in the
133 absence of ciprofloxacin (Fig 1D) but reduced the MIC of ciprofloxacin by 48% (Fig 1E). EVs
134 reduced planktonic growth of SMC1585 in the presence of 0.02 µg/ml ciprofloxacin by 27%,
135 compared to 0.02 µg/ml ciprofloxacin alone (Fig 1F). Full 20-hour growth curves for EV-exposed
136 and vehicle exposed PA14 and SMC1585 in the presence and absence of 0.02 µg/ml
137 ciprofloxacin are shown in S1 Fig. In the presence of 0.02 µg/ml ciprofloxacin there was a
138 statistically significant difference in the growth curves of PA14 and SMC1585 with EVs
139 compared to controls for the last 4 hours of growth. Thus, the combination of EVs and
140 ciprofloxacin reduced the MIC of ciprofloxacin as well as the growth of PA14 and a clinical
141 isolate of *Pseudomonas* (SMC1585).
142

143 EVs increase the fluoroquinolone sensitivity of *P. aeruginosa* 144 by targeting MexHI-OpmD

145 To begin to elucidate the mechanism whereby EVs increased the sensitivity of *P. aeruginosa* to
146 ciprofloxacin we analyzed the proteome of *P. aeruginosa* that had been exposed to EVs or
147 vehicle control. EVs reduced the protein levels of all three subunits of the fluoroquinolone efflux

148 pump MexHI-OpmD (Table 1). Compared to control, EVs decreased protein levels of MexH by
149 48%, MexI by 50% and OpmD by 35%. Normalized peak intensities for each sample set as well
150 as average log2 fold changes and p-values for all 1619 detected proteins in *P. aeruginosa* are
151 provided as S1 Table. To determine whether a reduction of MexHI-OpmD alone increased
152 fluoroquinolone sensitivity, planktonic growth experiments were performed with a *mexGHI-*
153 *opmD* deletion strain of *P. aeruginosa* PAO1 and the parental PAO1 wild type strain. In the
154 presence of ciprofloxacin EVs significantly decreased planktonic growth of wild type PAO1 (Fig
155 2). By contrast, in the presence of ciprofloxacin, EVs had no significant effect on the *mexGHI-*
156 *opmD* deletion strain (Δ+EV). S2 Fig contains full 20-hour growth curves for the data shown in
157 Fig 2. Taken together, the data suggest that EVs increase *P. aeruginosa* ciprofloxacin sensitivity
158 by targeting and down-regulating the fluoroquinolone efflux pump MexHI-OpmD.
159
160 **Table 1. EVs significantly reduce the protein levels of all three subunits of the**
161 **fluoroquinolone efflux pump MexHI-OpmD.**

Uniprot ID	Locus	Name	Product	log2 FC	% decrease	P-value
A0A0H2ZGA2	PA14_09530	MexH	RND efflux membrane fusion protein	-0.93	-48	0.0008
A0A0H2ZGB3	PA14_09520	MexI	RND efflux transporter	-1.01	-50	0.0003
A0A0H2ZF64	PA14_09500	OpmD	outer membrane protein	-0.62	-35	0.0161

162
163 Protein level changes in *P. aeruginosa* exposed to EVs compared to vehicle controls. FC = fold
164 change, N = three biological replicates of EVs secreted by different AEC donors. Statistical
165 significance was determined with QPROT.
166

167 # Characterization of sRNA content of EVs

168 We previously found that EVs secreted by AEC deliver the miRNA let-7b-5p to *P. aeruginosa*,
169 where it reduced biofilm formation and increased sensitivity to beta-lactam antibiotics by
170 targeting key genes involved in biofilm formation and beta-lactam resistance (19). However, let-
171 7b-5p alone did not reduce protein levels of MexHI-OpmD. To determine whether a different
172 sRNA was responsible for the EV-mediated reduction in MexHI-OpmD protein levels and the
173 resulting increased sensitivity to fluoroquinolone antibiotics, we re-analyzed our existing RNA-
174 seq data (GSE174690) to identify sRNAs in EVs that are predicted to target MexHI-OpmD. The
175 alignment-based characterization of EV sRNA content showed that tRNA and tRNA like
176 fragments were the most abundant sequences in EVs, accounting for 65% of all aligned reads
177 (Table 2). To gain a better understanding of the sRNA content of EVs at the sequence level, we
178 generated count tables for unique sequences and filtered them for the most abundant unique
179 sequences with at least 20 nucleotide length and at least 100 counts in each sample. The
180 resulting 1346 sequences were aligned to homo sapiens using BLAST+ to obtain annotations
181 for the 909 most abundant unique sequences with 100% identity and coverage (S2 Table).
182 Collectively, these 909 unique sequences accounted for 60% of total reads detected in all 3
183 replicate samples. The sequences with the highest total count (listed at the top of S2 Table)
184 include many tRNA and lncRNA fragments.
185

186 **Table 2. Alignment-based characterization of EV sRNA content.**

RNA type	% of total reads
tRNA	46.0
tRNA like	19.0
RefSeq anti	16.5
RefSeq	9.9

rfam	3.0
rRNA	1.8
other ncRNA	1.4
piRNA	1.1
lncRNA	0.7
miRNA	0.3
lncRNA anti	0.3
other ncRNA anti	0.1
CDBox	0.003

RNA types (column 1) and their relative abundance as a percentage of total reads (column 2). EVs were derived from three individual AEC donors. tRNA = transfer RNA, RefSeq = messenger RNA, anti = antisense, rfam = non-coding RNA annotated in Rfam database, rRNA = ribosomal RNA, ncRNA = non-coding RNA, piRNA = Piwi-interacting RNA, lncRNA = long non-coding RNA, miRNA = microRNA, CDBox = Small nucleolar RNA (snoRNA).

Transfer of EV sRNAs to *P. aeruginosa*

We previously described the transfer of miRNAs secreted in AEC EVs to *P. aeruginosa* (19). To assess the transfer of other sRNAs besides miRNAs to *P. aeruginosa*, we re-analyzed RNA-seq data of EV-exposed *P. aeruginosa* and unexposed controls (GSE174710). We generated count tables of unique sequences from trimmed reads for individual samples - three unexposed controls and three samples of *P. aeruginosa* exposed to EVs secreted by different AEC donors. Reads were filtered to include only sequences with a length of at least 20 nucleotides that were detected in all three EV-exposed *P. aeruginosa* samples and none of the unexposed control samples. Filtering on these criteria yielded 1022 sequences, 15 of which were perfect matches to human sequences in a BLAST search. The length requirement of at least 20 nucleotides was

204 chosen because shorter sequences tend to be less specific and map to many different regions
205 in the genome. The 15 human EV sRNA sequences listed in Table 3 were detected in EV-
206 exposed *P. aeruginosa*, but not in any of the unexposed control samples, suggesting that they
207 are delivered to *P. aeruginosa* by EVs. Subsequently, we used IntaRNA to predict target genes
208 of these 15 human EV sRNAs in *P. aeruginosa.*
209
210 **Table 3. Human EV RNA fragments delivered to *P. aeruginosa*.**

Sequence	Length	Description	Total Count	*mexH* Energy	*mexI* Energy	*opmD* Energy
TGGATTTTTGGAGCAGGGAG	20	CpG island DNA genomic Mse1 fragment	7	-13.19	-15.07	-17.44
AAATGGATTTTTGGAGCAGGGAG	**23**	**LHRI_LNC217 lncRNA**	**24**	**-13.18**	**-15.06**	**-17.43**
AAATGGATTTTTGGAGCAGGG	21	LHRI_LNC217 lncRNA	9	-8.68	-15.46	-16.97
GCATTGGTGGTTCAGTGGTAGAATTCTCGCCTG	**33**	**tRNA-Gly-GCC**	**11**	**-9.16**	**-14.77**	**-15.15**
GCGGCGTCCGGTGAGCTCTCGCTGGCC	**27**	**external transcribed spacer 18S ribosomal RNA**	**11**	**-10.52**	**-15.68**	**-14.77**
TGAGGTAGGAGGTTGTATAGTT	22	microRNA hsa-let-7e-5p (mature)	28	-10.01	-13.55	-14.6
TGAGGTAGTAGGTTGTATGGTT	22	microRNA let-7c-5p (mature)	21	-11.61	-13.67	-11.3

CAGGGATAACTGGCTTGTGGCGGCCAAG	28	external transcribed spacer 18S ribosomal RNA	4	-9.29	-13.95	-10.94
TCCCACATGGTCTAGCGGTTAGGATTCCTGG	31	tRNA-Glu-TTC	5	-10.26	-14.27	-10.92
AGTAAGGTCAGCTAAATAAGCTATCGGGCCCATACCCCGAAAATGTTGGTTATA	54	mitochondrial tRNA-fMet	6	-8.18	-10.98	-8.97
AGTAAGGTCAGCTAAATAAGCTATCGGGCCCATACCCCGAAAATGTTGGTTA	52	mitochondrial tRNA-fMet	8	-8.27	-10.96	-8.91
GAAAAAAAAAAAGGATGAGG	20	CKLF-like MARVEL transmembrane domain containing 6	7	-5.59	-9.04	-8.27
TGAGGTAGTAGATTGTATAGT	21	microRNA let-7f-5p, partial sequence (missing 3' T)	26	-7.59	-10.77	-7.83
CGCGACCTCAGATCAGACGTGGCG	24	external transcribed spacer 18S ribosomal RNA	6	-3.93	-5.8	-3.2
TCCCTGAGACCCTTTAACCTGT	22	miR-125a-5p, partial sequence	11	-8.78	-8.7	0

		(missing 3' GA)				

211

212 Listed are 15 human EV RNAs that were exclusively detected in EV-exposed *P. aeruginosa.*
213 Three sequences that were top candidates for follow-up experiments based on abundance and
214 targeting prediction for MexHI-OpmD are highlighted in bold font. Column 1 contains the sRNA
215 sequence, column 2 the sequence length in nucleotides (nt), column 3 the sequence identity as
216 determined with BLAST+, column 4 the total number of reads detected in *P. aeruginosa* after
217 EV exposure, and columns 5-7 the IntaRNA energy scores for *mexH*, *mexI* and *opmD*,
218 respectively. EVs were derived from three individual AEC donors.

219

220 Human EV sRNAs are predicted to target *P. aeruginosa* efflux 221 pump *mexHI-opmD*

222 To predict which *P. aeruginosa* genes the 15 human sRNAs that were delivered to *P.*
223 *aeruginosa* by EVs may target, the RNA-RNA interaction tool IntaRNA (50,51) was used to
224 calculate binding energy scores. The more negative the energy score, the higher the likelihood
225 of an RNA-RNA interaction. Table 3 lists the IntaRNA energy scores for each of the 15 EV
226 sRNAs for predicted targeting of the fluoroquinolone efflux pump subunits *mexH*, *mexI*, and
227 *opmD*. Three sRNAs with a high count in PA14+EV samples and the best (i.e., lowest) energy
228 scores for targeting of *mexH*, *mexI*, and *opmD* were selected for follow-up validation
229 experiments: a 23-nt lncRNA fragment, a 33-nt tRNA-Gly fragment and a 27-nt fragment of an
230 18S rRNA external transcribed spacer (highlighted in bold font in Table 3). As described next, of
231 the three top candidate sRNAs based on bioinformatic predictions, the rRNA fragment was
232 validated in wet lab experiments to increase the fluoroquinolone sensitivity of *P. aeruginosa* and
233 to decrease MexHI-OpmD protein levels.

234

235 # A human rRNA fragment mediates the increased
236 # fluoroquinolone sensitivity of *P. aeruginosa* by targeting
237 # MexHI-OpmD

238 To test whether the 18S rRNA spacer fragment in EVs mediates the increased ciprofloxacin
239 sensitivity of *P. aeruginosa* in response to EVs, we expressed the rRNA fragment (sequence
240 listed in Table 3) in *P. aeruginosa* using a plasmid with an arabinose-inducible promoter and
241 measured planktonic growth in the presence and absence of ciprofloxacin using the empty
242 vector as the control strain (ctrl). We observed that the rRNA fragment significantly decreased
243 planktonic growth of *P. aeruginosa* in the presence of ciprofloxacin (0.03 µg/ml, Fig 3A), while it
244 did not significantly alter planktonic growth in the absence of ciprofloxacin (Fig 3B).
245 Full 20-hour growth curves for the data in Fig 3A and 3B are provided in Fig S3. The rRNA
246 fragment also significantly decreased the MIC of *P. aeruginosa* for ciprofloxacin (Fig 3C), and
247 significantly reduced the number of live bacteria in the presence of ciprofloxacin (Fig 3D). In the
248 presence of the rRNA fragment planktonic growth of *P. aeruginosa* was reduced by 76%
249 compared to the empty vector control, the MIC of *P. aeruginosa* for ciprofloxacin was decreased
250 two-fold and the number of live bacteria was reduced by 73%.
251 To validate that the rRNA fragment increased the ciprofloxacin sensitivity of *P. aeruginosa* by
252 targeting the fluoroquinolone efflux pump MexHI-OpmD, we measured protein levels of MexHI-
253 OpmD in the presence and absence of the rRNA fragment and found that compared to the
254 empty vector control, the rRNA fragment decreased MexH by 53%, MexI by 26% and OpmD by
255 52% (Table 4). The decrease in the protein levels of MexH and OpmD was statistically
256 significant, and there was a trend for the rRNA fragment to decrease MexI protein levels that did
257 not quite reach statistical significance. Normalized peak intensities for each sample set as well
258 as average log2 fold changes and p-values for all 1911 detected proteins in *P. aeruginosa* are

259 provided as S3 Table. Taken together, these experiments demonstrate that the rRNA fragment
260 increased the ciprofloxacin sensitivity of *P. aeruginosa* by targeting the fluoroquinolone efflux
261 pump MexHI-OpmD.
262
263 **Table 4. A human rRNA fragment significantly reduces protein levels of MexH and OpmD.**

Uniprot ID	Locus	Name	Product	log2 FC	% decrease	p-value
A0A0H2ZGA2	PA14_09530	MexH	RND efflux membrane fusion protein	-1.09	-53	0.0003
A0A0H2ZGB3	PA14_09520	MexI	RND efflux transporter	-0.43	-26	0.1344
A0A0H2ZF64	PA14_09500	OpmD	outer membrane protein	-1.07	-52	0.0107

264
265 Protein level changes in a *P. aeruginosa* strain induced with 100 mM arabinose to express the
266 rRNA fragment compared to the empty vector control strain. FC = fold change, N = three
267 different clones of each strain. Statistical significance was determined with QPROT.
268
269
270 # Discussion
271
272 We report that AECs secrete EVs containing lncRNA, tRNA and 18S rRNA external transcribed
273 spacer fragments that are transferred to *P. aeruginosa*, and that EVs increased the
274 fluoroquinolone sensitivity of *P. aeruginosa* by reducing protein levels of the drug efflux pump
275 MexHI-OpmD. An 18S rRNA external transcribed spacer fragment by itself significantly reduced
276 the protein levels of MexH and OpmD, thereby increasing antibiotic sensitivity to ciprofloxacin.
277 The finding that AEC EVs contain rRNA fragments is consistent with prior characterizations of
278 the sRNA content of EVs secreted by airway epithelial cells (40,41). It has been previously
279 described that rRNA fragments are produced in a controlled manner that is population-, sex-

280 and tissue-specific, suggesting they constitute another class of small non-coding regulatory
281 RNAs (52,53). Several reports predict and speculate about a regulatory function of rRNA
282 derived fragments (52,54,55), with some studies providing evidence for the regulation of various
283 biological functions by rRNA fragments. Chen et al. report RNAi knockdown of an endogenous
284 20-nt 28S rRNA fragment in the human non-small cell lung carcinoma cell line H1299 induced
285 apoptosis and inhibited cell proliferation (56), while Wei et al. found that endogenous rRNA
286 fragments detected in human and murine liver regulate glucose metabolism in the murine
287 hepatoma cell line Hepa 1-6 and are differentially expressed in the livers of diabetic mice (57).
288 Moreover, several studies show co-immunoprecipitation of eukaryotic rRNA fragments with
289 Argonaute proteins (54,57,58), further corroborating our conclusion that rRNA fragments are
290 involved in the regulation of gene expression. Most of the previously described rRNA fragments
291 are derived from 5.8S, 18S or 28S rRNA as well as the internal transcribed spacer and, in fact,
292 some sequences that had been previously classified as miRNAs or piRNAs are in fact rRNA-
293 derived (53). There is very limited knowledge about the existence and function of fragments
294 derived from the rRNA external transcribed spacer. Lee et al. describe upregulation of rRNA
295 external transcribed spacer fragments in *Neurospora crassa* in response to DNA damage (59),
296 while Gupta et al. found that fragments derived from an rRNA external transcribed spacer are
297 upregulated in the parasitic protist *Entamoeba histolytica* in response to growth stress,
298 suggesting that these fragments play a regulatory role in the stress response (60). However,
299 direct evidence for the regulation of gene or protein expression by rRNA external transcribed
300 spacer fragments has not been published. In addition, to our knowledge there are no studies
301 showing cross kingdom transfer of rRNA fragments from human EVs to a bacterial pathogen,
302 nor is anything known about the effect of human rRNA fragments on bacterial gene expression.
303 Thus, to our knowledge, our data represent the first report of an rRNA fragment secreted by a
304 eukaryotic cell that regulates protein expression and alters the phenotype of a prokaryotic
305 organism. The exact mechanism of action and potential protein binding partners of rRNA

306 fragments in prokaryotes are beyond the scope of this work and need to be elucidated in future
307 studies.
308 We found that some, but not all, of the most abundant sequences in EVs can be detected in *P.*
309 *aeruginosa* following EV exposure. However, some human EV sRNA sequences detected in
310 EV-exposed *P. aeruginosa* are not among the most abundant EV sequences, suggesting
311 differential stability in *P. aeruginosa*. While RNA contained within EVs is protected from
312 degradation by extracellular RNases, once the EV RNA cargo is delivered to *P. aeruginosa,*
313 RNA that is not protected by binding to protein or *P. aeruginosa* mRNA targets may be more
314 prone to degradation, explaining the discrepancy between abundance in EVs compared to the
315 abundance after delivery to *P. aeruginosa* for some of the sRNAs.
316 One limitation of our study is that we did not assess other AEC EV cargo such as DNA, protein,
317 lipids, or metabolites, which could contribute to EV induced sensitivity to ciprofloxacin. However,
318 our experiment expressing the rRNA fragment in *P. aeruginosa* demonstrates that the rRNA
319 fragment alone is sufficient to reduce the abundance of MexH and OpmD and to increase the
320 sensitivity to ciprofloxacin.
321 Another limitation is that due to redundancy of fluoroquinolone efflux pumps in *P. aeruginosa*,
322 the suppression of MexHI-OpmD only leads to a partial effect on fluoroquinolone sensitivity.
323 MexEF-OprN serves as another fluoroquinolone efflux pump in *P. aeruginosa* (61), and there
324 are several additional efflux pumps that can serve this function (62), which helps explain why
325 deletion of MexHI-OpmD does not result in a more drastic increase in fluoroquinolone sensitivity
326 (Fig 2). On the other hand, as shown in Fig 2, the downregulation of MexHI-OpmD by EVs is
327 enough to reduce fluoroquinolone sensitivity to a level achieved with a complete deletion of the
328 efflux pump. Moreover, we found that expressing the rRNA fragment by itself led to a larger
329 reduction in *P. aeruginosa* planktonic growth in the presence of ciprofloxacin than EVs, and that
330 while both EVs and the rRNA fragment alone led to a protein level reduction of the
331 fluoroquinolone efflux pump MexHI-Opm, the rRNA fragment significantly suppressed additional

332 proteins involved in mediating fluoroquinolone resistance, including MexA, GyrA , and ParC
333 (62,63). This may explain the increased ability of the rRNA fragment to reduce planktonic
334 growth in the presence of ciprofloxacin compared to EVs, which contain additional cargo that
335 may counteract the effect of the rRNA fragment.
336 *P. aeruginosa* in the lung is exposed to EVs secreted by other cell types in addition to those
337 secreted by AEC, most notably immune cells like neutrophils and macrophages, whose EV RNA
338 content may include the rRNA fragment in our study as well as other sRNAs that may affect
339 antibiotic resistance of *Pseudomonas*. Therefore, a final limitation is that our study cannot
340 elucidate the cumulative effect that EV sRNAs from multiple cell types would have on *P.*
341 *aeruginosa* in the lungs. However, re-analysis of publicly available data (GSE126051) from a
342 study characterizing sRNAs in human plasma (64) revealed that rRNA fragments that were
343 identical in length and sequence to the rRNA fragment described in this study were present in
344 plasma of healthy control subjects. Moreover, identical rRNA fragments were detected in EVs
345 isolated from human bronchoalveolar lavage fluid (BALF; Dr. Alix Ashare, personal
346 communication). These observations reveal the biological significance of our study since our
347 rRNA fragment was found in clinical samples and is not limited to our model system of primary
348 AECs. So far, there are no published studies that comprehensively characterize the sRNA
349 content of EVs isolated from human BALF, and, as noted in a recent review by Zareba et al.,
350 future in-depth RNA-seq profiling of distinct EV populations in BALF will elucidate their role in
351 disease pathogenesis and provide insight into treatment strategies (65). The important
352 questions of whether *P. aeruginosa* exposure alters the sRNA content of AEC EVs and whether
353 there is a difference in the sRNA cargo of EVs secreted by WT and CF AEC need to be
354 addressed in future studies.
355 To assess whether EV sRNA targeting of efflux pumps is limited to *P. aeruginosa* or extends to
356 efflux pump orthologs in other common lung pathogens we utilized IntaRNA to predict targeting
357 of *Burkholderia cenocepacia* (which has orthologs for *mexH*, *mexI* and *opmD*) and

358 *Staphylococcus aureus* (which has an ortholog for *mexI*). Our candidate rRNA spacer fragment
359 is predicted to target orthologs of *mexI* and *opmD* in *Burkholderia cenocepacia*, suggesting that
360 AEC EV sRNAs are likely to affect other lung pathogens beyond *P. aeruginosa* and warrant
361 future analysis beyond the scope of the current study.
362 In summary, our study provides the first evidence for transfer of lncRNA, tRNA and rRNA
363 fragments from eukaryotic EVs to a prokaryote and provides direct evidence for regulation of the
364 prokaryote by a eukaryotic rRNA fragment, resulting in subsequent phenotypic alterations such
365 as increased fluoroquinolone sensitivity. The development of new treatment approaches utilizing
366 a combination of human rRNA fragments and antibiotics in nanoparticles or EVs may benefit
367 individuals with chronic antibiotic-resistant *P. aeruginosa* infections.
368
369

370 Materials and Methods

371

372 Culture of airway epithelial cells and EV isolation

373 De-identified primary human AEC were obtained from Dr. Scott Randell (University of North
374 Carolina, Chapel Hill, NC) and cultured in BronchiaLife basal medium (Lifeline Cell Technology,
375 Frederick, MD, Cat. # LM-0007) supplemented with the BronchiaLife B/T LifeFactors Kit (Lifeline
376 Cell Technology, Cat. # LS-1047) as well as 10,000 U/ml Penicillin and 10,000 µg/ml
377 Streptomycin (Sigma-Aldrich, Cat. # P4333), as previously described (66). EVs were isolated
378 from AEC culture supernatants (passages 4-8) with the ExoQuick-TC EV isolation kit (System
379 Biosciences, Palo Alto, CA, Cat. # EXOTC50A-1) and characterized as previously described
380 (67).
381

382 ## Bacterial strains and culture

383 For all experiments, *P. aeruginosa* strains PA14, PAO1, and the mucoid CF clinical isolate
384 SMC1585 (49) were cultured in Luria broth (LB, Thermo Fisher Scientific, Waltham, MA). A
385 deletion mutant for the fluoroquinolone efflux pump *mexGHI*-opmD in the PAO1 background
386 (strain DW101, PAO1ΔGHID), as well as the matching parental PAO1 wild type strain, were
387 generously provided by Dr. Helen Zgurskaya from the University of Oklahoma (61). Deletion of
388 *opmD* in the PAO1*ΔmexGHI*-opmD strain was confirmed by PCR. Briefly, RNA was isolated
389 from PAO1*ΔmexGHI-opmD* and the parental PAO1 wild type strain using the miRNeasy Mini Kit
390 (Qiagen, Germantown, MD, Cat. # 217004), cDNA was synthesized with the Invitrogen
391 RETROscript Reverse Transcription Kit (Thermo Fisher Scientific Cat. # 10585595), and the
392 presence of *opmD* was interrogated by PCR amplification using the following primers: forward
393 5'-CCTGGTGGAGTTTCTTCGAC-3' and reverse 5'- CGTCGTAGTCCAGCTGTTGT-3'.
394 *P. aeruginosa* strains expressing either the 18S rRNA spacer fragment under the control of an
395 arabinose-inducible promoter or the empty vector control were produced by transforming PA14
396 with a pMQ70 expression vector (68) containing either the rRNA fragment sequence (listed in
397 Table 3) as an insert, or no insert (control). Strains were cultured with 300 µg/ml carbenicillin
398 (Sigma-Aldrich, Cat. # C1389) to select for bacteria containing the plasmid and 100 mM L-(+)-
399 arabinose (Sigma-Aldrich, St. Louis, MO, Cat. # A3256) was added during experiments to
400 induce expression of the rRNA fragment.
401

402 ## Bacterial growth curves and CFU count

403 The minimal inhibitory concentration (MIC) of the fluoroquinolone antibiotic ciprofloxacin was
404 determined by incubation of each *P. aeruginosa* strain with 8 different concentrations of
405 ciprofloxacin (0-0.25 µg/ml) in triplicate for 20 hours in a plate reader at 37°C. The OD600 was
406 recorded every 15 minutes and the MIC for ciprofloxacin was calculated by fitting the growth

407 curve data with a Gompertz function, as previously described (69,70). At the beginning of the
408 20-hour growth curves, 5000 colony forming units (CFUs) of *P. aeruginosa* were exposed to
409 $5x10^9$ EV/ml, corresponding to a concentration of EVs measured in AEC culture supernatants
410 by us, as well as in human bronchoalveolar lavage fluid (42,71). During exposure of *P.*
411 *aeruginosa* to EVs, ciprofloxacin (Sigma-Aldrich, Cat. # 17850-5G-F) was present in the culture
412 medium at a concentration equivalent to one-third to one-half the MIC of a given strain, as
413 indicated in the figure legends. CFU/ml for viable planktonic bacteria were obtained by dilution
414 plating of supernatants.
415

416 Proteomics of *P. aeruginosa*

417 $1.5*10^7$ CFUs of PA14 were exposed to $1.5*10^{10}$ EV isolated from AEC from three donors or
418 vehicle controls for a PA14:EV ratio of 1:1000 and incubated for 15 h at 37°C at 225 rpm.
419 Samples were processed and TMT labeled as described previously (19). All six samples were
420 run in duplicate, peak intensities from duplicate runs were averaged and filtered to retain 1619
421 proteins that were detected in all replicate samples. Differentially abundant proteins were
422 identified using QPROT (72). The mass spectrometry proteomics data have been deposited to
423 the ProteomeXchange Consortium (73) via the MassIVE (74) partner repository with the dataset
424 identifier PXD033213.
425 In addition, following overnight cultures with 300 µg/ml carbenicillin to select for bacteria with the
426 plasmid containing the rRNA fragment or the empty plasmid, 3 different clones of the PA14
427 strains expressing either the rRNA fragment or the empty vector control were cultured with 100
428 mM arabinose for 15 h at 37°C at 225 rpm to induce expression of the rRNA fragment. Cell
429 pellets were washed with PBS, lysed and proteins (200 µg of each sample) were purified by
430 acetone/trichloroacetic acid precipitation overnight at -20°C. After washing the pellet with ice-
431 cold acetone, the resulting protein pellet was resuspended in 50 µL of 8 M urea in 400 mM

432 ammonium bicarbonate, pH 7.8, reduced with 4 mM dithiothreitol at 50°C for 30 minutes, and
433 cysteines were alkylated with 18 mM iodoacetamide for 30 minutes. The solution was then
434 diluted to <2 M urea and trypsin (Promega, Madison, WI) was added at a final trypsin/protein
435 ratio of 1:100 prior to overnight incubation at 37°C. The resulting peptides were desalted using
436 solid-phase extraction on a C18 Spin column and eluted in 240 µL of 80% acetonitrile in 0.1%
437 formic acid. All samples were analyzed in technical duplicates by LC-MS/MS using a nanoElute
438 coupled to a timsTOF Pro Mass Spectrometer (Bruker Daltonics). Two hundred nanogram of
439 each digested peptide sample was loaded on a capillary C18 column (25 cm length, 75 µm
440 inner diameter, 1.6 µm particle size, 120 Å pore size; IonOpticks). The flow rate was kept at 300
441 nL/min. Solvent A was 0.1% FA in water, and Solvent B was 0.1% FA in ACN. The peptides
442 were separated on a 100 min analytical gradient from 2% ACN/0.1% FA to 35% ACN/0.1% FA
443 for a total of 120 min gradient. The timsTOF Pro was operated in the PASEF mode. MS and
444 MS/MS spectra were acquired from 100-1700 m/z. The inverse reduced ion mobility $1/K_0$ was
445 set to 0.60−1.60 V·s/cm^2 over a ramp time of 100 ms. Data-dependent acquisition was
446 performed using 10 PASEF MS/MS scans per cycle with a near 100% duty cycle. The resulting
447 protein tandem MS data was queried for protein identification and label-free quantification
448 against the Uniprot *Pseudomonas aeruginosa* strain UCBPP-PA14 database (proteome ID
449 UP000000653, retrieved on Feb 2, 2022) using MaxQuant v2.0.3.1. The following modifications
450 were set as search parameters: peptide mass tolerance at 20 ppm, trypsin digestion cleavage
451 after K or R (except when followed by P), 2 allowed missed cleavage sites,
452 carbamidomethylated cysteine (static modification), and oxidized methionine, deaminated
453 asparagine/glutamine, and protein N-term acetylation (variable modification). Search results
454 were validated with peptide and protein FDR both at 0.01. LFQ intensities were averaged
455 across technical replicates, filtered to retain 1911 proteins detected in at least two replicate
456 samples, and normalized prior to QPROT analysis (72). The mass spectrometry proteomics

457 data have been deposited to the ProteomeXchange Consortium (73) via the PRIDE (75) partner
458 repository with the dataset identifier PXD033165.
459

460 Characterization of EV sRNA content

461 Previously, we characterized the miRNA content of AEC EVs (19); here, we focus on the EV
462 sRNA content beyond miRNAs. The raw data as well as count tables of aligned reads provided
463 by System Biosciences can be accessed through NCBI's Gene Expression Omnibus (GEO
464 Series accession number GSE174690). In addition to the alignment-based characterization we
465 also performed a sequence-based characterization of EV sRNA content. Adaptor trimming of
466 raw reads was performed with fastp version 0.20.0 (76). Trimmed reads from EVs secreted by
467 three donors of AEC yielded close to 500,000 unique sequences, about 40,000 of which were
468 detected in all three biological replicates. Count tables with the number of reads per sample for
469 each unique sequence were generated using the Unix command “cat fastp.fastq.gz | gunzip |
470 awk '(NR%4==2)' | sort | uniq -c | sort -k 1 -n”. To determine the origin of the most abundant
471 unique EV sRNA sequences, we ran command line BLAST+ (77) for 1346 sequences that had
472 a minimum of 100 counts per sample and a length of at least 20 nucleotides. Arguments to the
473 blastn function included -taxids 9606 (homo sapiens), -perc_identity 100 (requiring a perfect
474 match), -qcov_hsp_perc 100 (requiring 100% query coverage) and -task blastn-short (to adjust
475 for a short input sequence). Genbank accessions returned by BLAST were annotated using the
476 R package rentrez (78). Subsequently, RNA-seq samples from EV-exposed *P. aeruginosa* were
477 used to assess whether human sRNAs are transferred to *P. aeruginosa* by EVs.
478

479 RNA-seq to detect transfer of EV RNA to *P. aeruginosa*

480 Existing RNA-seq data of *P. aeruginosa* exposed to PBS vehicle control in triplicate or to EVs
481 from 3 AEC donors (19) was re-analyzed to identify EV-mediated transfer of sRNA other than

482 miRNAs to *P. aeruginosa.* The raw data can be accessed through NCBI's Gene Expression
483 Omnibus (GEO Series accession number GSE174710). For each sample, trimmed reads were
484 compiled into count tables of unique sequences and samples were filtered for unique
485 sequences of at least 20 nucleotides in length that were contained in all three EV-exposed *P.*
486 *aeruginosa* samples, but none of the control samples. The origin of 1022 unique sequences
487 matching these criteria was determined using BLAST+ (77), as described above, and included a
488 separate alignment to -taxids 287 (*P. aeruginosa*). Genbank accessions returned by BLAST
489 were annotated using the R package rentrez (78). For EV RNA sequences that were of human
490 origin, we generated IntaRNA targeting predictions (50,51) for *P. aeruginosa* genes, as
491 described below.
492

493 IntaRNA target predictions

494 We used the IntaRNA algorithm (50,51) to predict whether human sRNAs transferred to *P.*
495 *aeruginosa* by EVs might regulate *P. aeruginosa* gene expression by targeting bacterial
496 mRNAs. *P. aeruginosa* UCBPP-PA14 reference sequences and standard parameters were
497 used to obtain energy scores as a measure of the likelihood of RNA-RNA interaction based on
498 sequence similarity. The more negative the energy score, the higher the likelihood of interaction.
499 Three top candidate RNA fragments derived from a lncRNA, a tRNA, and an rRNA were
500 selected based on predicted targeting of MexHI-OpmD and abundance in *P. aeruginosa*
501 following EV exposure. To assess whether targeting predictions extend beyond *P. aeruginosa* to
502 other common lung pathogens, we ran IntaRNA to predict targeting of MexHI-OpmD orthologs
503 by our top candidate RNA fragments in *Burkholderia cenocepacia* J2315, a multidrug-resistant
504 CF clinical isolate, and *Staphylococcus aureus* COL, a MRSA clinical isolate.
505

506 ## Statistical Analysis

507 Data were analyzed with Prism 8 for macOS (version 9.3.1, Graphpad, San Diego, CA)
508 and the R software environment for statistical computing and graphics version 4.1.1 (79) using
509 appropriate statistical methods, as indicated in the figure legends. Statistically significant
510 differences between bacterial growth curves were determined with permutation tests using the
511 compareGrowthCurves function from the R package statmod (version 1.4.36) (80,81).
512
513

514 # Acknowledgements

515 The authors would like to thank Dr. Helen Zgurskaya (University of Oklahoma) for providing the
516 PAO1 deletion mutant for the fluoroquinolone efflux pump *mexGHI*-opmD as well as the matching
517 parental PAO1 wild type strain. Mass Spectrometry analyses of the rRNA fragment expressing
518 and empty vector strain of *P. aeruginosa* were performed by the Mass Spectrometry Technology
519 Access Center at McDonnell Genome Institute (MTAC@MGI) at Washington University School
520 of Medicine.
521

522 # Figures

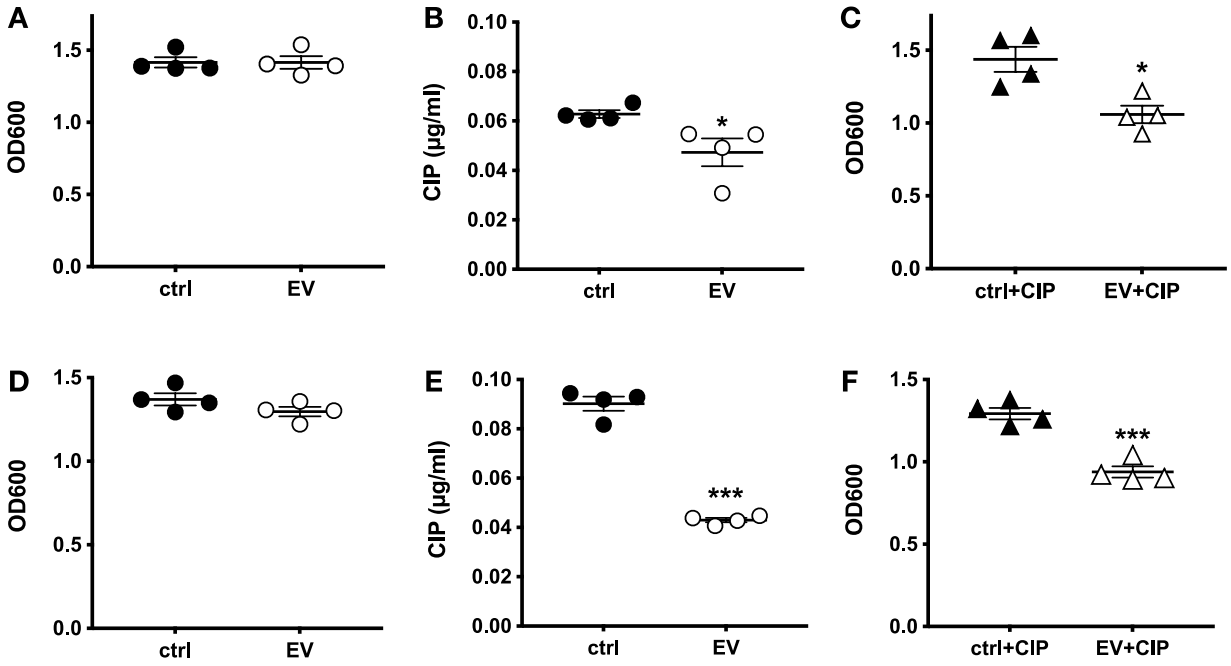

523

524 **Fig 1. EVs increase the fluoroquinolone sensitivity of *P. aeruginosa*.**

525 EVs did not significantly affect planktonic growth (OD600) of PA14 in the absence of
526 ciprofloxacin (CIP) after a 20-hour incubation (A), but significantly reduced the MIC of
527 ciprofloxacin (B) as well as planktonic growth of PA14 in the presence of 0.02 µg/ml
528 ciprofloxacin (C). EVs did not significantly affect planktonic growth (OD600) of the clinical isolate
529 SMC1585 in the absence of ciprofloxacin after a 20-hour incubation (D), but significantly
530 reduced the MIC of ciprofloxacin (E) as well as planktonic growth in the presence of 0.02 µg/ml
531 ciprofloxacin (F). Statistical significance was determined using unpaired t-tests. EVs were
532 isolated from four AEC donors and each data point is the mean of three technical replicates
533 from each donor. ***$P < 0.001$, *$P < 0.05$.

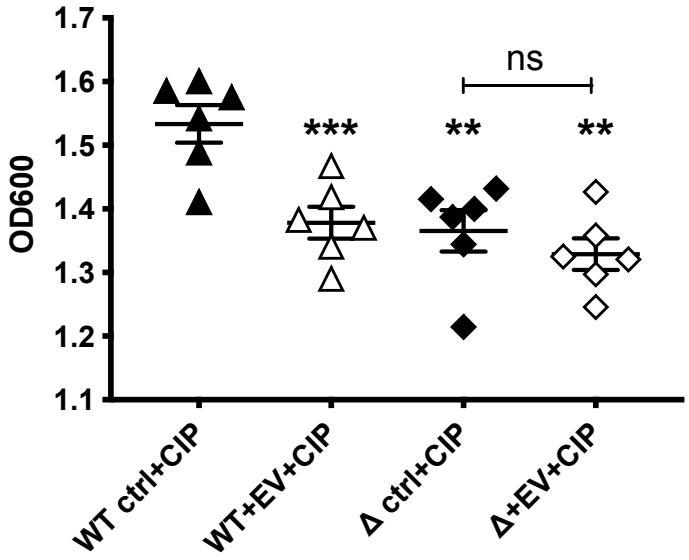

534

535

536 **Fig 2. EVs increase *P. aeruginosa* ciprofloxacin sensitivity by targeting the**

537 **fluoroquinolone efflux pump MexHI-OpmD.** EVs decreased planktonic growth of wild type

538 (WT) PAO1 in the presence of ciprofloxacin (0.03 μg/ml). EVs in the presence of ciprofloxacin

539 (0.03 μg/ml) had no significant effect on the *mexHI-opmD* knockout strain (Δ+EV). Statistical

540 significance was determined with repeated measures one-way ANOVA followed by Dunnett's

541 multiple comparisons test. EVs were isolated from six AEC donors and each data point is the

542 mean of three technical replicates from each donor. ***P < 0.001 compared to WT ctrl, **P <

543 0.01 compared to WT ctrl, ns = not significant.

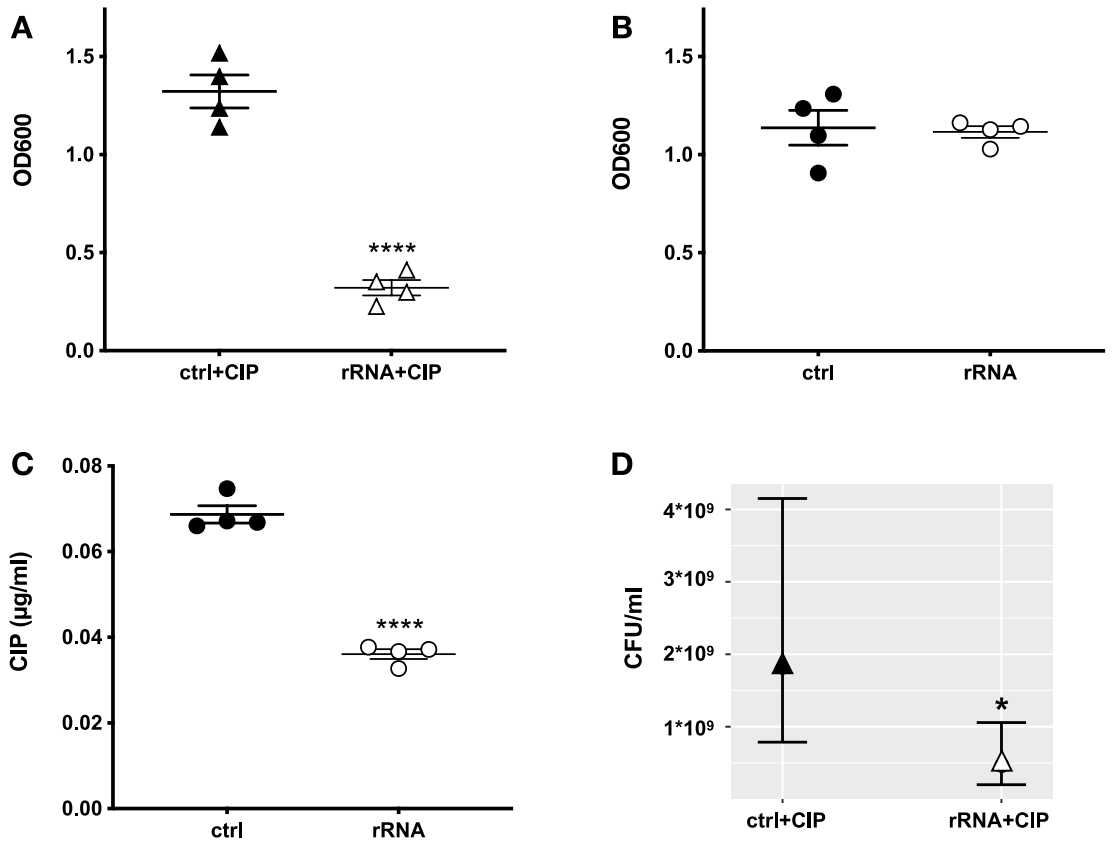

544

545 **Fig 3. A human rRNA fragment increases the fluoroquinolone sensitivity of *P.***
546 ***aeruginosa*.** Compared to the empty vector control (ctrl), the rRNA fragment significantly
547 reduced planktonic growth (OD600) of PA14 in the presence of 0.03 µg/ml ciprofloxacin (CIP)
548 and 100 mM arabinose after a 20-hour incubation (A) but did not significantly affect planktonic
549 growth in the absence of ciprofloxacin (B). The rRNA fragment also significantly reduced the
550 minimal inhibitory concentration (MIC) of ciprofloxacin (C) as well as the number of live bacteria
551 in the presence of 0.03 µg/ml ciprofloxacin (D). Statistical significance was determined using
552 unpaired t-tests for panels A-C with N = four independent experiments using different clones of
553 each strain and each data point is the mean of three technical replicates and a negative
554 binomial regression model for panel D with N = three independent experiments using different
555 clones of each strain. Panel D shows the batch-corrected estimates from the regression model.
556 CFU = colony forming units. ****P < 0.0001 compared to ctrl, *P < 0.05 compared to ctrl.

557 **Supporting information**

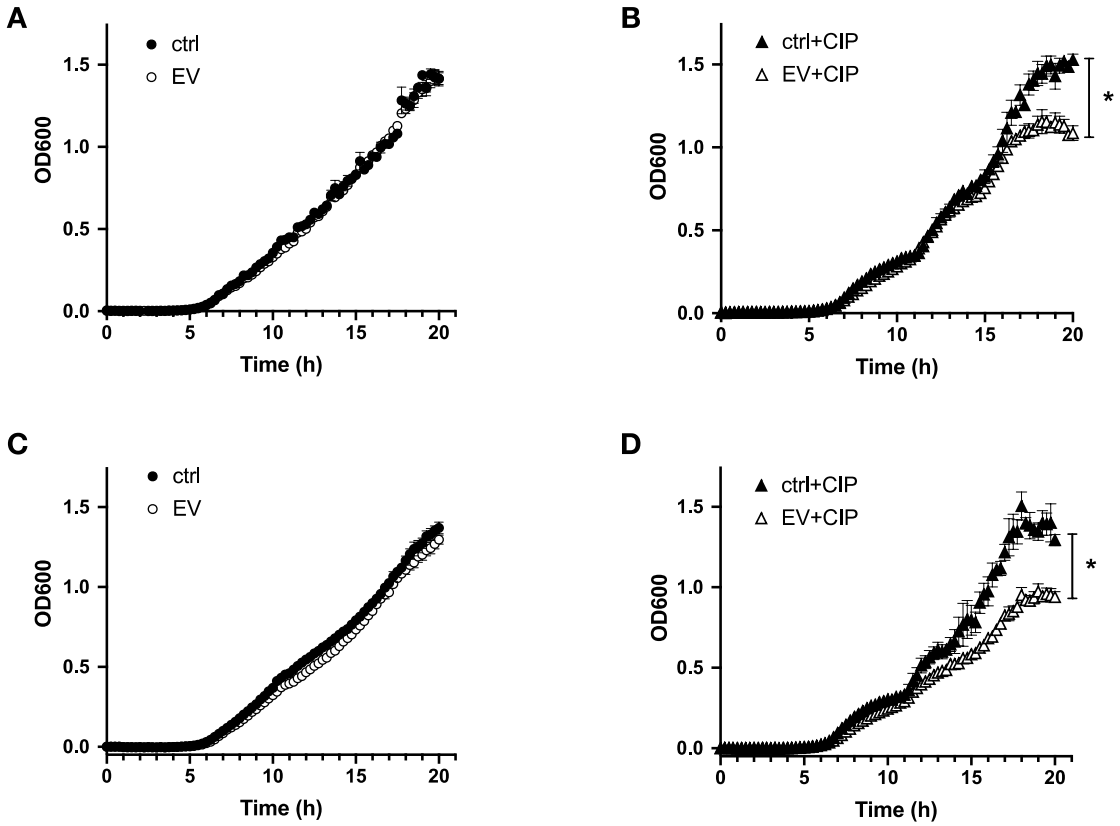

558

559 **S1 Fig. EVs increase the fluoroquinolone sensitivity of *P. aeruginosa*.**

560 (A) 20-hour planktonic growth curves (OD600) of PA14 exposed to EVs or vehicle control (ctrl)
561 in the absence of ciprofloxacin. There was no significant difference between the growth curves
562 for the last 4 hours of growth. (B) 20-hour planktonic growth curves (OD600) of PA14 exposed
563 to 0.02 µg/ml ciprofloxacin and EVs or 0.02 µg/ml ciprofloxacin and vehicle control (ctrl). There
564 was a significant difference between the growth curves for the last 4 hours of growth. (C) 20-
565 hour planktonic growth curves (OD600) of clinical isolate SMC1585 exposed to EVs or vehicle
566 control (ctrl) in the absence of ciprofloxacin. There was no significant difference between the
567 growth curves for the last 4 hours of growth. (D) 20-hour planktonic growth curves (OD600) of
568 clinical isolate SMC1585 exposed to 0.02 µg/ml ciprofloxacin and EVs or 0.02 µg/ml

569 ciprofloxacin and vehicle control (ctrl). There was a significant difference between the growth
570 curves for the last 4 hours of growth. Each data point shows the mean +/- SEM of EVs isolated
571 from four AEC donors (or matching controls), averaged across three technical replicates.
572 Statistical significance was determined using permutation tests. * $P < 0.05$.

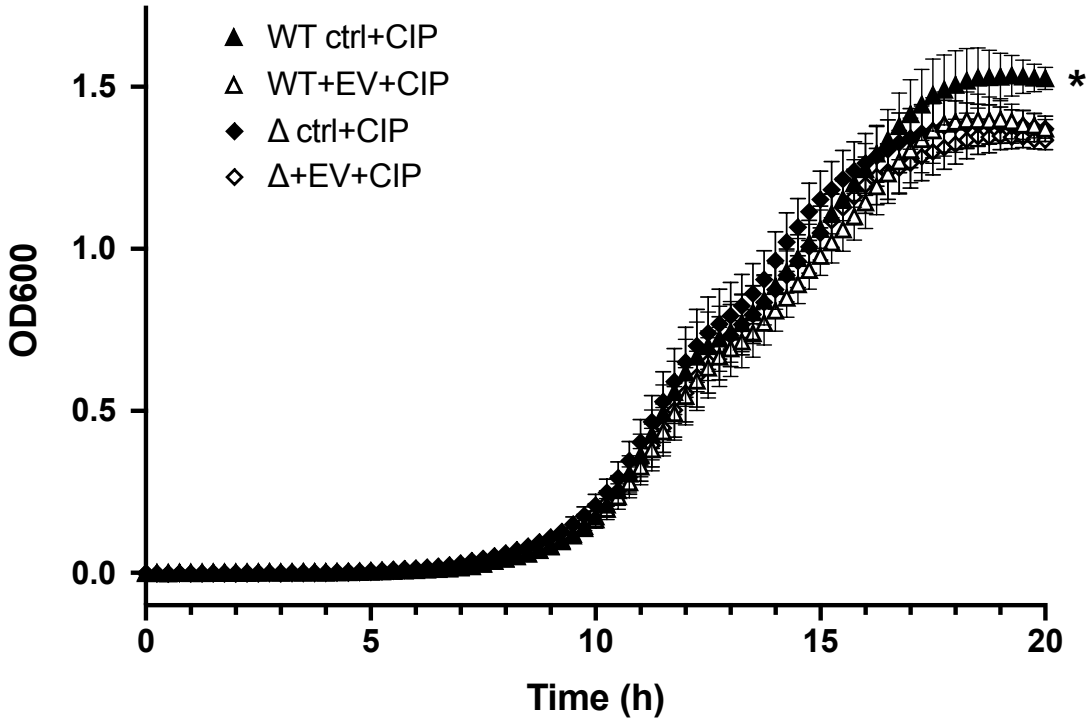

573

574

575 **S2 Fig. EVs increase *P. aeruginosa* ciprofloxacin sensitivity by targeting the**

576 **fluoroquinolone efflux pump MexHI-OpmD.** 20-hour planktonic growth curves (OD600) of

577 PAO1 wild type (WT) and the PAO1 *mexHI-opmD* knockout strain (Δ) exposed to 0.03 μg/ml

578 ciprofloxacin (CIP) in the presence and absence of EVs. There was a significant difference

579 between WT ctrl+CIP and all other growth curves for the last hour of growth, while here was no

580 significant difference between the other three growth curves. Each data point shows the mean

581 +/- SEM of EVs isolated from six AEC donors (or matching controls), averaged across three

582 technical replicates. Statistical significance was determined using permutation tests. * $P < 0.05$.

583

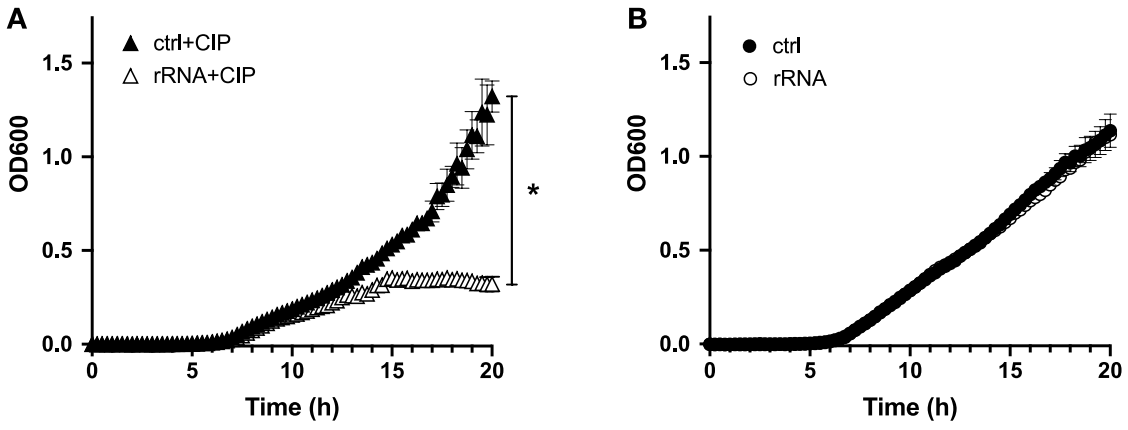

584

585 **S3 Fig. A human rRNA fragment increases the fluoroquinolone sensitivity of *P.***

586 ***aeruginosa*.** (A) 20-hour planktonic growth curves (OD600) of PA14 expressing the rRNA

587 fragment or empty vector control (ctrl) in the presence of 0.03 μg/ml ciprofloxacin (CIP) and 100

588 mM arabinose. There was a significant difference between the growth curves for the empty

589 vector control (ctrl) and the rRNA expressing strain. (B) There was no significant difference in

590 the 20-hour planktonic growth curves (OD600) of PA14 expressing the rRNA fragment or empty

591 vector control in the absence of ciprofloxacin. Each data point shows the mean +/- SEM from

592 four different clones of each strain averaged across three technical replicates. Statistical

593 significance was determined using permutation tests. * $P < 0.05$.

594

595 **S1 Table. Proteomics data of EV-exposed *P. aeruginosa* and unexposed controls.**
596 Normalized peak intensities for each sample as well as average log2 fold changes and p-values
597 for 1619 proteins that were detected in duplicate runs of all six samples. EVs were derived from
598 three individual AEC donors.
599
600 **S2 Table. Origin of most abundant sRNAs from the sequence-based characterization of**
601 **EV sRNA content.** 909 most abundant unique sequences with at least 100 counts per sample
602 accounted for 60% of total reads for sequences detected in all 3 replicate samples. Listed are
603 the nucleotide sequence (column 1), sequence length (column 2), number of reads in EVs
604 (column 3) and origin of sequence as determined with BLAST+ (column 4). EVs were derived
605 from three individual AEC donors.
606
607 **S3 Table. Proteomics data of *P. aeruginosa* expressing the rRNA fragment compared to**
608 **empty vector controls.** Normalized peak intensities for each sample as well as average log2
609 fold changes and p-values for 1911 proteins that were detected in at least two of three replicate
610 samples.

611 **References**

612 1. Behzadi P, Baráth Z, Gajdács M. It's Not Easy Being Green: A Narrative Review on the
613 Microbiology, Virulence and Therapeutic Prospects of Multidrug-Resistant Pseudomonas
614 aeruginosa. Antibiotics (Basel) [Internet]. 2021 Jan 4 [cited 2021 Apr 12];10(1). Available
615 from: https://www.ncbi.nlm.nih.gov/pmc/articles/PMC7823828/

616 2. Chong WH, Saha BK, Ananthakrishnan Ramani, Chopra A. State-of-the-art review of
617 secondary pulmonary infections in patients with COVID-19 pneumonia. Infection. 2021
618 Mar 11;1–15.

619 3. Giacobbe DR, Battaglini D, Enrile EM, Dentone C, Vena A, Robba C, et al. Incidence and
620 Prognosis of Ventilator-Associated Pneumonia in Critically Ill Patients with COVID-19: A
621 Multicenter Study. J Clin Med [Internet]. 2021 Feb 3 [cited 2021 Apr 12];10(4). Available
622 from: https://www.ncbi.nlm.nih.gov/pmc/articles/PMC7913191/

623 4. Qu J, Cai Z, Liu Y, Duan X, Han S, Liu J, et al. Persistent Bacterial Coinfection of a
624 COVID-19 Patient Caused by a Genetically Adapted Pseudomonas aeruginosa Chronic
625 Colonizer. Front Cell Infect Microbiol. 2021;11:641920.

626 5. Yang S, Hua M, Liu X, Du C, Pu L, Xiang P, et al. Bacterial and fungal co-infections
627 among COVID-19 patients in intensive care unit. Microbes Infect [Internet]. 2021 Mar 5
628 [cited 2021 Apr 12]; Available from:
629 https://www.ncbi.nlm.nih.gov/pmc/articles/PMC7933791/

630 6. Bullington W, Hempstead S, Smyth AR, Drevinek P, Saiman L, Waters VJ, et al.
631 Antimicrobial resistance: Concerns of healthcare providers and people with CF. Journal of
632 Cystic Fibrosis [Internet]. 2020 Jun 17 [cited 2021 Apr 12]; Available from:
633 https://www.sciencedirect.com/science/article/pii/S1569199320301594

634 7. López-Causapé C, Rojo-Molinero E, Macià MD, Oliver A. The problems of antibiotic
635 resistance in cystic fibrosis and solutions. Expert Review of Respiratory Medicine. 2015
636 Jan 2;9(1):73–88.

637 8. Tchakal-Mesbahi A, Metref M, Singh VK, Almpani M, Rahme LG. Characterization of
638 antibiotic resistance profiles in Pseudomonas aeruginosa isolates from burn patients. Burns.
639 2021 Mar 17;

640 9. Baiou A, Elbuzidi AA, Bakdach D, Zaqout A, Alarbi KM, Bintaher AA, et al. Clinical
641 characteristics and risk factors for the isolation of multi-drug-resistant Gram-negative
642 bacteria from critically ill patients with COVID-19. J Hosp Infect. 2021 Apr;110:165–71.

643 10. CDC. Antibiotic Resistance Threats in the United States, 2019. 2019;150.

644 11. Koeppen K, Hampton TH, Jarek M, Scharfe M, Gerber SA, Mielcarz DW, et al. A Novel
645 Mechanism of Host-Pathogen Interaction through sRNA in Bacterial Outer Membrane
646 Vesicles. PLoS Pathog. 2016 Jun;12(6):e1005672.

647 12. Blenkiron C, Simonov D, Muthukaruppan A, Tsai P, Dauros P, Green S, et al.
648 Uropathogenic Escherichia coli Releases Extracellular Vesicles That Are Associated with
649 RNA. PLOS ONE. 2016;16.

650 13. Choi J-W, Kim S-C, Hong S-H, Lee H-J. Secretable Small RNAs via Outer Membrane
651 Vesicles in Periodontal Pathogens. J Dent Res. 2017 Apr 1;96(4):458–66.

652 14. Lefebvre FA, Lécuyer E. Small Luggage for a Long Journey: Transfer of Vesicle-Enclosed
653 Small RNA in Interspecies Communication. Front Microbiol [Internet]. 2017 Mar 16 [cited
654 2021 Apr 12];8. Available from:
655 http://journal.frontiersin.org/article/10.3389/fmicb.2017.00377/full

656 15. Lee H-J. Microbe-Host Communication by Small RNAs in Extracellular Vesicles: Vehicles
657 for Transkingdom RNA Transportation. Int J Mol Sci. 2019 Mar 25;20(6).

658 16. Munhoz da Rocha IF, Amatuzzi RF, Lucena ACR, Faoro H, Alves LR. Cross-Kingdom
659 Extracellular Vesicles EV-RNA Communication as a Mechanism for Host–Pathogen
660 Interaction. Front Cell Infect Microbiol. 2020 Nov 18;10:593160.

661 17. Lécrivain A-L, Beckmann BM. Bacterial RNA in extracellular vesicles: A new regulator of
662 host-pathogen interactions? Biochimica et Biophysica Acta (BBA) - Gene Regulatory
663 Mechanisms. 2020 Jul 1;1863(7):194519.

664 18. Zhang H, Zhang Y, Song Z, Li R, Ruan H, Liu Q, et al. sncRNAs packaged by Helicobacter
665 pylori outer membrane vesicles attenuate IL-8 secretion in human cells. International
666 Journal of Medical Microbiology. 2020 Jan 1;310(1):151356.

667 19. Koeppen K, Nymon A, Barnaby R, Bashor L, Li Z, Hampton TH, et al. Let-7b-5p in
668 vesicles secreted by human airway cells reduces biofilm formation and increases antibiotic
669 sensitivity of P. aeruginosa. Proc Natl Acad Sci U S A. 2021 Jul 13;118(28):e2105370118.

670 20. Vojtech L, Woo S, Hughes S, Levy C, Ballweber L, Sauteraud RP, et al. Exosomes in
671 human semen carry a distinctive repertoire of small non-coding RNAs with potential
672 regulatory functions. Nucleic Acids Res. 2014 Jun;42(11):7290–304.

673 21. Chiou N-T, Kageyama R, Ansel KM. Selective Export into Extracellular Vesicles and
674 Function of tRNA Fragments during T Cell Activation. Cell Reports. 2018
675 Dec;25(12):3356-3370.e4.

676 22. Abramowicz A, Story MD. The Long and Short of It: The Emerging Roles of Non-Coding
677 RNA in Small Extracellular Vesicles. Cancers. 2020 Jun 2;12(6):1445.

678 23. Garcia-Silva MR, Cabrera-Cabrera F, Güida MC, Cayota A. Hints of tRNA-Derived Small
679 RNAs Role in RNA Silencing Mechanisms. Genes (Basel). 2012 Oct 10;3(4):603–14.

680 24. Lee YS, Shibata Y, Malhotra A, Dutta A. A novel class of small RNAs: tRNA-derived
681 RNA fragments (tRFs). Genes Dev. 2009 Nov 15;23(22):2639–49.

682 25. Kumar P, Anaya J, Mudunuri SB, Dutta A. Meta-analysis of tRNA derived RNA fragments
683 reveals that they are evolutionarily conserved and associate with AGO proteins to recognize
684 specific RNA targets. BMC Biol [Internet]. 2014 Oct 1 [cited 2021 Apr 13];12. Available
685 from: https://www.ncbi.nlm.nih.gov/pmc/articles/PMC4203973/

686 26. Raina M, Ibba M. tRNAs as regulators of biological processes. Front Genet [Internet]. 2014
687 Jun 11 [cited 2021 Apr 13];5. Available from:
688 https://www.ncbi.nlm.nih.gov/pmc/articles/PMC4052509/

689 27. Avcilar-Kucukgoze I, Kashina A. Hijacking tRNAs From Translation: Regulatory
690 Functions of tRNAs in Mammalian Cell Physiology. Front Mol Biosci. 2020;7:610617.

691 28. Anderson P, Ivanov P. tRNA fragments in human health and disease. FEBS Lett. 2014 Nov
692 28;588(23):4297–304.

693 29. Xie Y, Yao L, Yu X, Ruan Y, Li Z, Guo J. Action mechanisms and research methods of
694 tRNA-derived small RNAs. Signal Transduction and Targeted Therapy. 2020 Jun
695 30;5(1):1–9.

696 30. Ogawa Y, Taketomi Y, Murakami M, Tsujimoto M, Yanoshita R. Small RNA
697 Transcriptomes of Two Types of Exosomes in Human Whole Saliva Determined by Next
698 Generation Sequencing. Biological & Pharmaceutical Bulletin. 2013;36(1):66–75.

699 31. Fatima F, Nawaz M. Vesiculated Long Non-Coding RNAs: Offshore Packages Deciphering
700 Trans-Regulation between Cells, Cancer Progression and Resistance to Therapies. Non-
701 Coding RNA. 2017 Mar;3(1):10.

702 32. Li Z, Stanton BA. Transfer RNA-Derived Fragments, the Underappreciated Regulatory
703 Small RNAs in Microbial Pathogenesis. Front Microbiol. 2021;12:687632.

704 33. Stanton BA. Extracellular Vesicles and Host-Pathogen Interactions: A Review of Inter-
705 Kingdom Signaling by Small Noncoding RNA. Genes (Basel). 2021 Jun 30;12(7):1010.

706 34. Fujita Y, Kosaka N, Araya J, Kuwano K, Ochiya T. Extracellular vesicles in lung
707 microenvironment and pathogenesis. Trends in Molecular Medicine. 2015 Sep;21(9):533–
708 42.

709 35. Fujita Y, Kadota T, Araya J, Ochiya T, Kuwano K. Extracellular Vesicles: New Players in
710 Lung Immunity. Am J Respir Cell Mol Biol. 2018 May;58(5):560–5.

711 36. Hough KP, Chanda D, Duncan SR, Thannickal VJ, Deshane JS. Exosomes in
712 immunoregulation of chronic lung diseases. Allergy. 2017 Apr;72(4):534–44.

713 37. McVey MJ, Maishan M, Blokland KEC, Bartlett N, Kuebler WM. Extracellular vesicles in
714 lung health, disease, and therapy. Am J Physiol Lung Cell Mol Physiol. 2019 Jun
715 1;316(6):L977–89.

716 38. He S, Chen D, Hu M, Zhang L, Liu C, Traini D, et al. Bronchial epithelial cell extracellular
717 vesicles ameliorate epithelial–mesenchymal transition in COPD pathogenesis by alleviating
718 M2 macrophage polarization. Nanomedicine: Nanotechnology, Biology and Medicine.
719 2019 Jun;18:259–71.

720 39. Stachowiak Z, Wojsyk-Banaszak I, Jończyk-Potoczna K, Narożna B, Langwiński W,
721 Kycler Z, et al. MiRNA Expression Profile in the Airways Is Altered during Pulmonary
722 Exacerbation in Children with Cystic Fibrosis—A Preliminary Report. J Clin Med
723 [Internet]. 2020 Jun 16 [cited 2021 Apr 15];9(6). Available from:
724 https://www.ncbi.nlm.nih.gov/pmc/articles/PMC7356328/

725 40. Chahar HS, Corsello T, Kudlicki AS, Komaravelli N, Casola A. Respiratory Syncytial
726 Virus Infection Changes Cargo Composition of Exosome Released from Airway Epithelial
727 Cells. Sci Rep [Internet]. 2018 Jan 10 [cited 2021 Apr 14];8. Available from:
728 https://www.ncbi.nlm.nih.gov/pmc/articles/PMC5762922/

729 41. Corsello T, Kudlicki AS, Garofalo RP, Casola A. Cigarette Smoke Condensate Exposure
730 Changes RNA Content of Extracellular Vesicles Released from Small Airway Epithelial
731 Cells. Cells. 2019 Dec 17;8(12).

732 42. Armstrong DA, Nymon AB, Ringelberg CS, Lesseur C, Hazlett HF, Howard L, et al.
733 Pulmonary microRNA profiling: implications in upper lobe predominant lung disease. Clin
734 Epigenetics [Internet]. 2017 May 30 [cited 2021 Apr 6];9. Available from:
735 https://www.ncbi.nlm.nih.gov/pmc/articles/PMC5450072/

736 43. Gon Y, Shimizu T, Mizumura K, Maruoka S, Hikichi M. Molecular techniques for
737 respiratory diseases: MicroRNA and extracellular vesicles. Respirology. 2020
738 Feb;25(2):149–60.

739 44. Guiot J, Struman I, Louis E, Louis R, Malaise M, Njock M-S. Exosomal miRNAs in Lung
740 Diseases: From Biologic Function to Therapeutic Targets. J Clin Med [Internet]. 2019 Aug
741 29 [cited 2021 Apr 15];8(9). Available from:
742 https://www.ncbi.nlm.nih.gov/pmc/articles/PMC6781233/

743 45. Liu S, da Cunha AP, Rezende RM, Cialic R, Wei Z, Bry L, et al. The Host Shapes the Gut
744 Microbiota via Fecal MicroRNA. Cell Host & Microbe. 2016 Jan;19(1):32–43.

745 46. Liu S, Rezende RM, Moreira TG, Tankou SK, Cox LM, Wu M, et al. Oral Administration
746 of miR-30d from Feces of MS Patients Suppresses MS-like Symptoms in Mice by
747 Expanding Akkermansia muciniphila. Cell Host Microbe. 2019 Dec 11;26(6):779-794.e8.

748 47. Teng Y, Ren Y, Sayed M, Hu X, Lei C, Kumar A, et al. Plant-Derived Exosomal
749 MicroRNAs Shape the Gut Microbiota. Cell Host Microbe. 2018 Nov 14;24(5):637-652.e8.

750 48. Heijerman H, Westerman E, Conway S, Touw D, Döring G, consensus working group.
751 Inhaled medication and inhalation devices for lung disease in patients with cystic fibrosis:
752 A European consensus. J Cyst Fibros. 2009 Sep;8(5):295–315.

753 49. Moreau-Marquis S, Coutermarsh B, Stanton BA. Combination of hypothiocyanite and
754 lactoferrin (ALX-109) enhances the ability of tobramycin and aztreonam to eliminate
755 Pseudomonas aeruginosa biofilms growing on cystic fibrosis airway epithelial cells. J
756 Antimicrob Chemother. 2015 Jan;70(1):160–6.

757 50. Busch A, Richter AS, Backofen R. IntaRNA: efficient prediction of bacterial sRNA targets
758 incorporating target site accessibility and seed regions. Bioinformatics. 2008 Dec
759 15;24(24):2849–56.

760 51. Mann M, Wright PR, Backofen R. IntaRNA 2.0: enhanced and customizable prediction of
761 RNA–RNA interactions. Nucleic Acids Res. 2017 Jul 3;45(Web Server issue):W435–9.

762 52. Cherlin T. Ribosomal RNA fragmentation into short RNAs (rRFs) is modulated in a sex-
763 and population of origin-specific manner. 2020;19.

764 53. Lambert M, Benmoussa A, Provost P. Small Non-Coding RNAs Derived From Eukaryotic
765 Ribosomal RNA. ncRNA. 2019 Feb 4;5(1):16.

766 54. Guan L, Grigoriev A. Age-Related Argonaute Loading of Ribosomal RNA Fragments.
767 MIRNA. 2020 Mar 4;9(2):142–52.

768 55. Guan L, Grigoriev A. Computational meta-analysis of ribosomal RNA fragments: potential
769 targets and interaction mechanisms. Nucleic Acids Research. 2021 Apr 19;49(7):4085–103.

770 56. Chen Z, Sun Y, Yang X, Wu Z, Guo K, Niu X, et al. Two featured series of rRNA-derived
771 RNA fragments (rRFs) constitute a novel class of small RNAs. Xue Y, editor. PLoS ONE.
772 2017 Apr 25;12(4):e0176458.

773 57. Wei H, Zhou B, Zhang F, Tu Y, Hu Y, Zhang B, et al. Profiling and Identification of Small
774 rDNA-Derived RNAs and Their Potential Biological Functions. Müller M, editor. PLoS
775 ONE. 2013 Feb 13;8(2):e56842.

776 58. Czech B, Malone CD, Zhou R, Stark A, Schlingeheyde C, Dus M, et al. An endogenous
777 small interfering RNA pathway in Drosophila. Nature. 2008 Jun 5;453(7196):798–802.

778 59. Lee H-C, Chang S-S, Choudhary S, Aalto AP, Maiti M, Bamford DH, et al. qiRNA, a new
779 type of small interfering RNA induced by DNA damage. Nature. 2009 May
780 14;459(7244):274–7.

781 60. Gupta AK, Panigrahi SK, Bhattacharya A, Bhattacharya S. Self-circularizing 5′-ETS RNAs
782 accumulate along with unprocessed pre ribosomal RNAs in growth-stressed Entamoeba
783 histolytica. Sci Rep. 2012 Dec;2(1):303.

784 61. Wolloscheck D, Krishnamoorthy G, Nguyen J, Zgurskaya HI. Kinetic control of quorum
785 sensing in Pseudomonas aeruginosa by multidrug efflux pumps. ACS Infect Dis. 2018 Feb
786 9;4(2):185–95.

787 62. Lister PD, Wolter DJ, Hanson ND. Antibacterial-Resistant *Pseudomonas aeruginosa* :
788 Clinical Impact and Complex Regulation of Chromosomally Encoded Resistance
789 Mechanisms. Clin Microbiol Rev. 2009 Oct;22(4):582–610.

790 63. Rehman A, Patrick WM, Lamont IL. Mechanisms of ciprofloxacin resistance in
791 Pseudomonas aeruginosa: new approaches to an old problem. Journal of Medical
792 Microbiology. 2019 Jan 1;68(1):1–10.

793 64. Giraldez MD, Spengler RM, Etheridge A, Goicochea AJ, Tuck M, Choi SW, et al.
794 Phospho-RNA-seq: a modified small RNA-seq method that reveals circulating mRNA and
795 lncRNA fragments as potential biomarkers in human plasma. EMBO J [Internet]. 2019 Jun
796 3 [cited 2021 Apr 16];38(11). Available from:
797 https://onlinelibrary.wiley.com/doi/10.15252/embj.2019101695

798 65. Zareba L, Szymanski J, Homoncik Z, Czystowska-Kuzmicz M. EVs from BALF-Mediators
799 of Inflammation and Potential Biomarkers in Lung Diseases. Int J Mol Sci. 2021 Apr
800 1;22(7).

801 66. Fulcher ML, Randell SH. Human nasal and tracheo-bronchial respiratory epithelial cell
802 culture. Methods Mol Biol. 2013;945:109–21.

803 67. Koeppen K, Nymon AB, Barnaby R, Li Z, Hampton TH, Ashare A, et al. CF Monocyte
804 Derived Macrophages Have an Attenuated Response to Extracellular Vesicles Secreted by
805 Airway Epithelial Cells. Am J Physiol Lung Cell Mol Physiol. 2021 Jan 20;

806 68. Shanks RMQ, Caiazza NC, Hinsa SM, Toutain CM, O'Toole GA. Saccharomyces
807 cerevisiae-based molecular tool kit for manipulation of genes from gram-negative bacteria.
808 Appl Environ Microbiol. 2006 Jul;72(7):5027–36.

809 69. Lambert RJW, Pearson J. Susceptibility testing: accurate and reproducible minimum
810 inhibitory concentration (MIC) and non-inhibitory concentration (NIC) values. Journal of
811 Applied Microbiology. 2000;88(5):784–90.

812 70. Malek AA, Wargo MJ, Hogan DA. Absence of Membrane Phosphatidylcholine Does Not
813 Affect Virulence and Stress Tolerance Phenotypes in the Opportunistic Pathogen
814 Pseudomonas aeruginosa. PLoS One [Internet]. 2012 Feb 17 [cited 2021 Apr 6];7(2).
815 Available from: https://www.ncbi.nlm.nih.gov/pmc/articles/PMC3281885/

816 71. Scheller N, Herold S, Kellner R, Bertrams W, Jung AL, Janga H, et al. Proviral
817 MicroRNAs Detected in Extracellular Vesicles From Bronchoalveolar Lavage Fluid of
818 Patients With Influenza Virus–Induced Acute Respiratory Distress Syndrome. The Journal
819 of Infectious Diseases. 2019 Jan 29;219(4):540–3.

820 72. Choi H, Kim S, Fermin D, Tsou C-C, Nesvizhskii AI. QPROT: statistical method for
821 testing differential expression using protein-level intensity data in label-free quantitative
822 proteomics. J Proteomics. 2015 Nov 3;129:121–6.

823 73. Deutsch EW, Bandeira N, Sharma V, Perez-Riverol Y, Carver JJ, Kundu DJ, et al. The
824 ProteomeXchange consortium in 2020: enabling "big data" approaches in proteomics.
825 Nucleic Acids Res. 2020 Jan 8;48(D1):D1145–52.

826 74. Wang M, Wang J, Carver J, Pullman BS, Cha SW, Bandeira N. Assembling the
827 Community-Scale Discoverable Human Proteome. Cell Syst. 2018 Oct 24;7(4):412-421.e5.

828 75. Perez-Riverol Y, Bai J, Bandla C, García-Seisdedos D, Hewapathirana S, Kamatchinathan
829 S, et al. The PRIDE database resources in 2022: a hub for mass spectrometry-based
830 proteomics evidences. Nucleic Acids Res. 2022 Jan 7;50(D1):D543–52.

831 76. Chen S, Zhou Y, Chen Y, Gu J. fastp: an ultra-fast all-in-one FASTQ preprocessor.
832 Bioinformatics. 2018 Sep 1;34(17):i884–90.

833 77. Camacho C, Coulouris G, Avagyan V, Ma N, Papadopoulos J, Bealer K, et al. BLAST+:
834 architecture and applications. BMC Bioinformatics. 2009 Dec 15;10:421.

835 78. Winter DJ. rentrez: An R package for the NCBI eUtils API. The R Journal. 2017;9(2):520–
836 6.

837 79. R Core Team. R: A language and environment for statistical computing. [Internet]. Vienna,
838 Austria: R Foundation for Statistical Computing; 2021. Available from: URL
839 https://www.R-project.org/

840 80. Baldwin T, Sakthianandeswaren A, Curtis JM, Kumar B, Smyth GK, Foote SJ, et al.
841 Wound healing response is a major contributor to the severity of cutaneous leishmaniasis in
842 the ear model of infection. Parasite Immunology. 2007;29(10):501–13.

843 81. Elso CM, Roberts LJ, Smyth GK, Thomson RJ, Baldwin TM, Foote SJ, et al. Leishmaniasis
844 host response loci (lmr1–3) modify disease severity through a Th1/Th2-independent
845 pathway. Genes Immun. 2004 Mar;5(2):93–100.

846